Supporting Information

Tunable Band Gap Photoluminescence from Atomically Thin Transition-Metal Dichalcogenide Alloys

Yanfeng Chen,[1,†] Jinyang Xi,[2,†] Dumitru O. Dumcenco,[3,†] Zheng Liu,[4] Kazu Suenaga,[4] Dong Wang,[2] Zhigang Shuai,[2] Ying-Sheng Huang,[3] and Liming Xie[1*]

[1]Key Laboratory of Standardization and Measurement for Nanotechnology of Chinese Academy of Sciences, National Center for Nanoscience and Technology, Beijing 100190, P. R. China

[2]Key Laboratory of Organic Optoelectronics and Molecular Engineering, Department of Chemistry, Tsinghua University, Beijing 100084, P. R. China

[3]Department of Electronic Engineering, National Taiwan University of Science and Technology, Taipei 106, Taiwan, Republic of China

[4]Nanotube Research Center, National Institute of Advanced Industrial Science and Technology (AIST), Tsukuba 305-8565, Japan

[†]These authors contributed equally to this work.

[*]To whom correspondence should be addressed: ~~xielm@nanoctr.cn~~

Table S1. EDX characterization results of $Mo_{1-x}W_xS_2$ single crystals.

$Mo_{1-x}W_xS_2$ samples	**nominal growth W content *x***	**EDX of W content *x***
MoS_2	0	0
$Mo_{0.87}W_{0.13}S_2$	0.1	0.13
$Mo_{0.80}W_{0.20}S_2$	0.2	0.20
$Mo_{0.71}W_{0.29}S_2$	0.3	0.29
$Mo_{0.58}W_{0.42}S_2$	0.4	0.42
$Mo_{0.47}W_{0.53}S_2$	0.5	0.53
$Mo_{0.39}W_{0.61}S_2$	0.6	0.61

$Mo_{0.34}W_{0.66}S_2$	0.7	0.66
$Mo_{0.23}W_{0.77}S_2$	0.8	0.77
$Mo_{0.12}W_{0.88}S_2$	0.9	0.88
WS_2	1	1

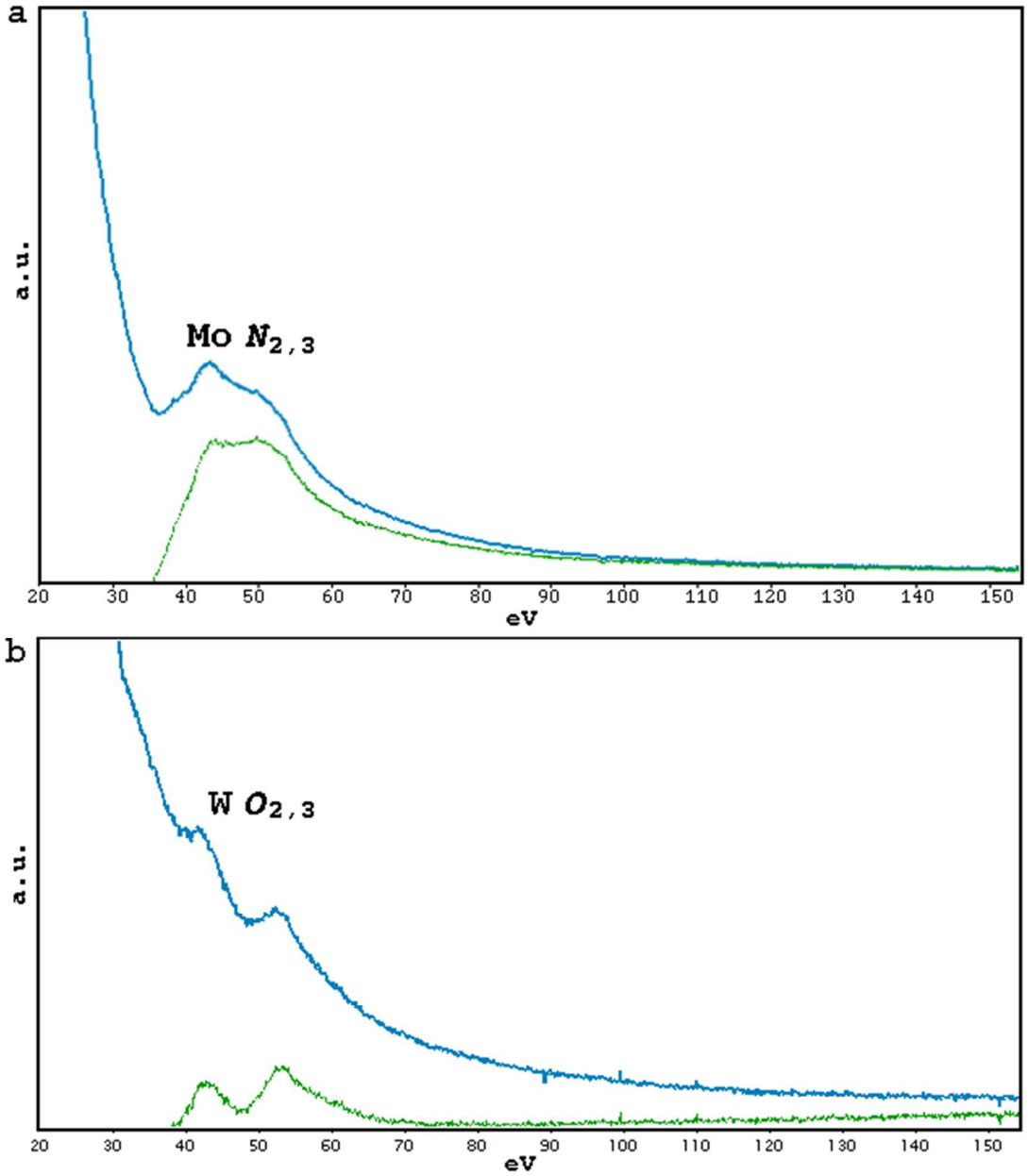

Figure S1. EELS of MoS_2 (top panel) and WS_2 (bottom panel). The blue lines are original EELS spectra and the green lines are spectra after background subtraction.

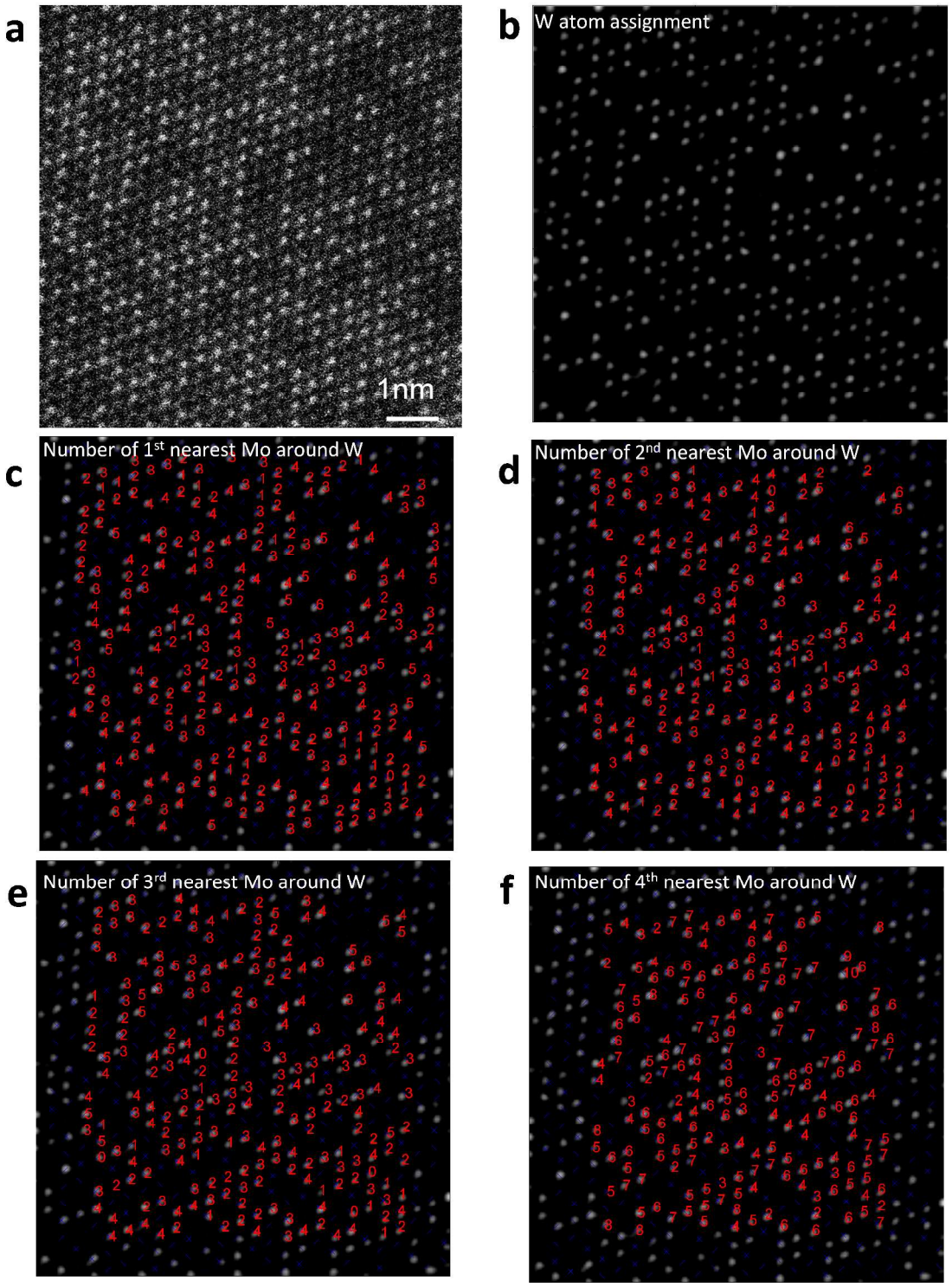

Figure S2. (a) STEM image of a $Mo_{0.47}W_{0.53}S_2$ monolayer (same as Fig 1b in the main text). (b) Image in panel (a) after FFT filtering and contrast-adjusting, only showing W atoms in bright spots. (c), (d), (e), (f) Images showing the numbers of 1st, 2nd, 3rd and 4th nearest Mo atoms around each W atoms, respectively. Blue crosses indicate metal atom

(Mo or W) positions. By averaging the numbers, α_i is calculated to be 0.01, -0.02, -0.03, 0.04 for i=1, 2, 3 and 4, respectively.

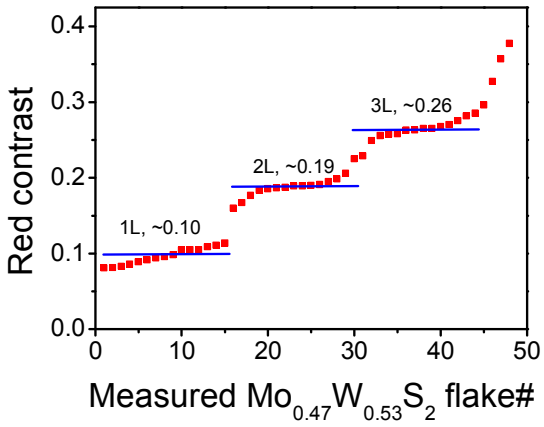

Figure S3. Red color contrast of $Mo_{0.47}W_{0.53}S_2$ flakes measured from optical images (totally 48 flakes). The plateaus at ~0.10, ~0.19 and ~0.26 were assigned to monolayers (1L), bilayers (2L) and trilayers (3L), respectively.

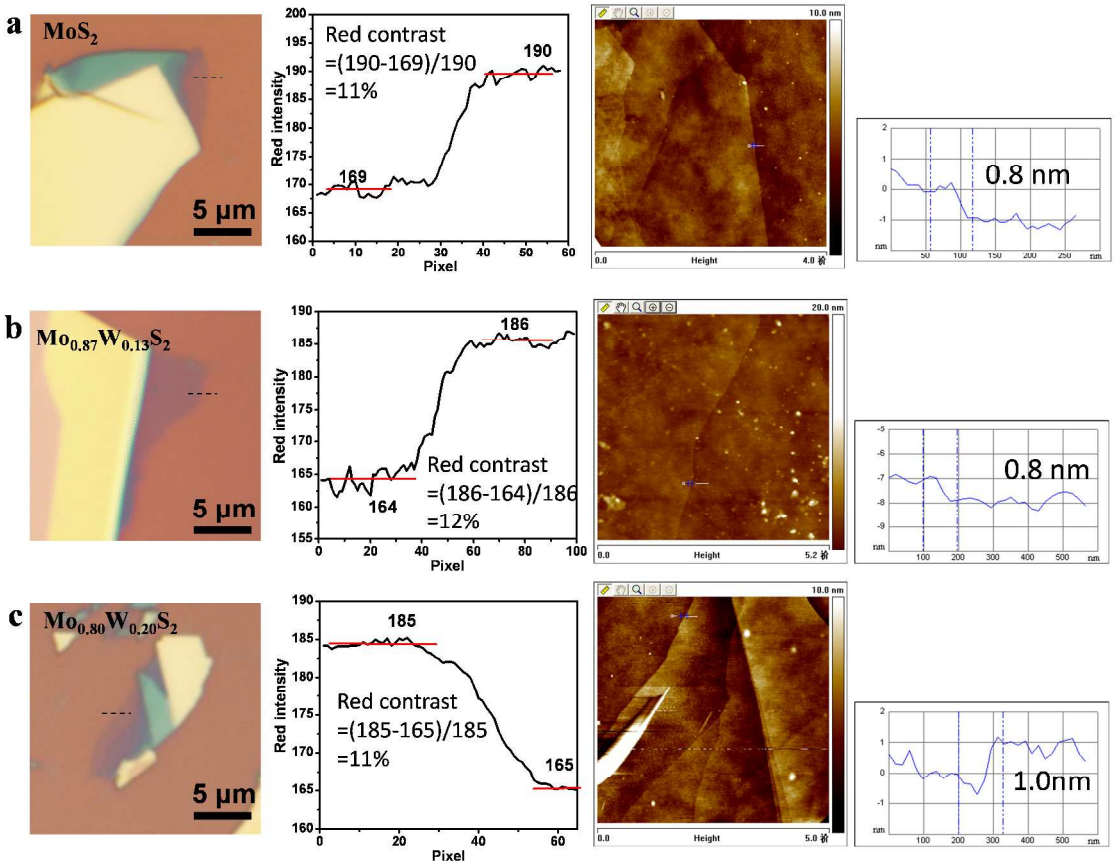

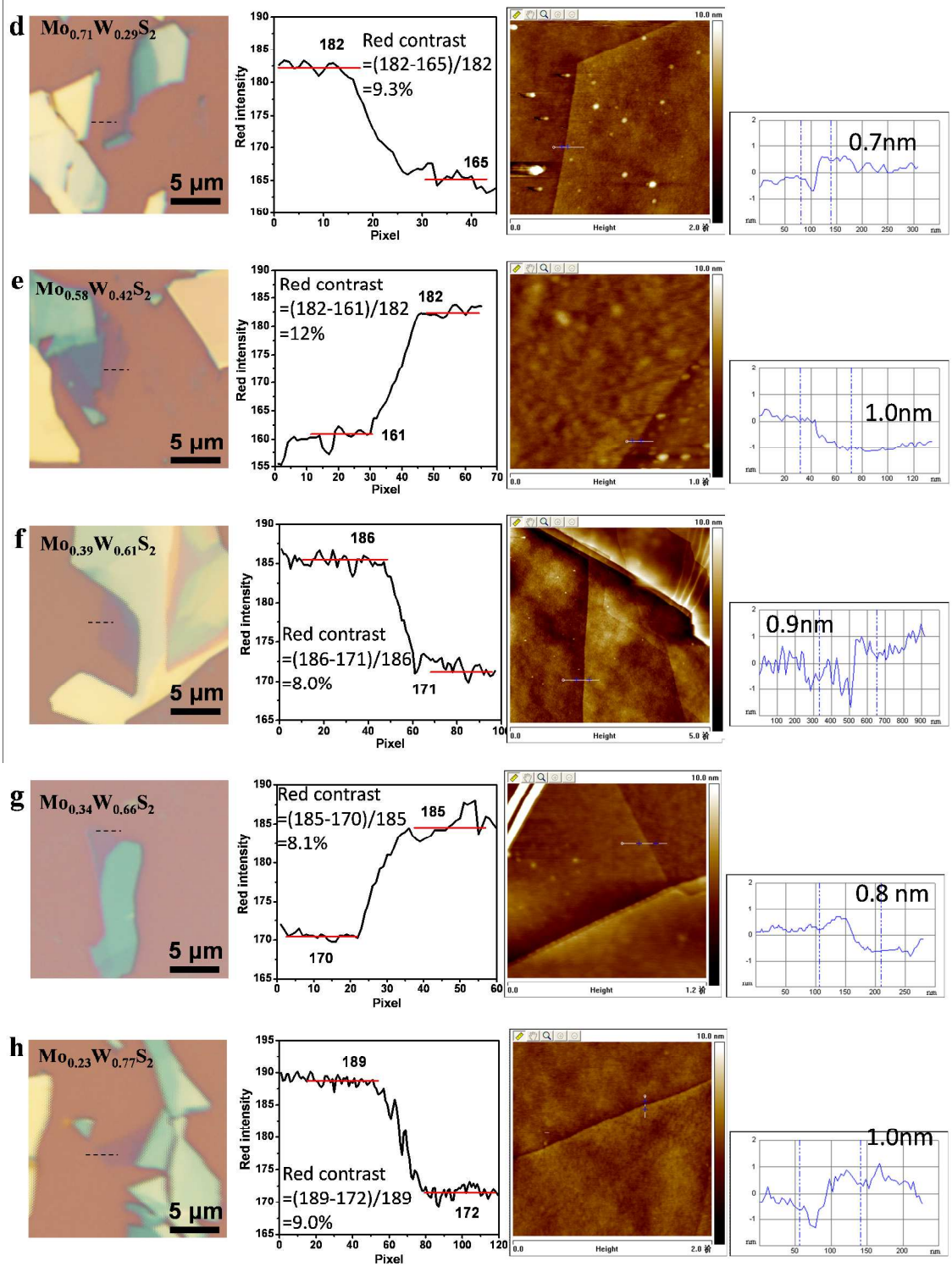
d
$Mo_{0.71}W_{0.29}S_2$
5 μm
182
Red contrast
=(182-165)/182
=9.3%
165
Red intensity
Pixel
0.7nm
e
$Mo_{0.58}W_{0.42}S_2$
5 μm
Red contrast
=(182-161)/182
=12%
182
161
Red intensity
Pixel
1.0nm
f
$Mo_{0.39}W_{0.61}S_2$
5 μm
186
Red contrast
=(186-171)/186
=8.0%
171
Red intensity
Pixel
0.9nm
g
$Mo_{0.34}W_{0.66}S_2$
5 μm
Red contrast
=(185-170)/185
=8.1%
185
170
Red intensity
Pixel
0.8 nm
h
$Mo_{0.23}W_{0.77}S_2$
5 μm
189
Red contrast
=(189-172)/189
=9.0%
172
Red intensity
Pixel
1.0nm

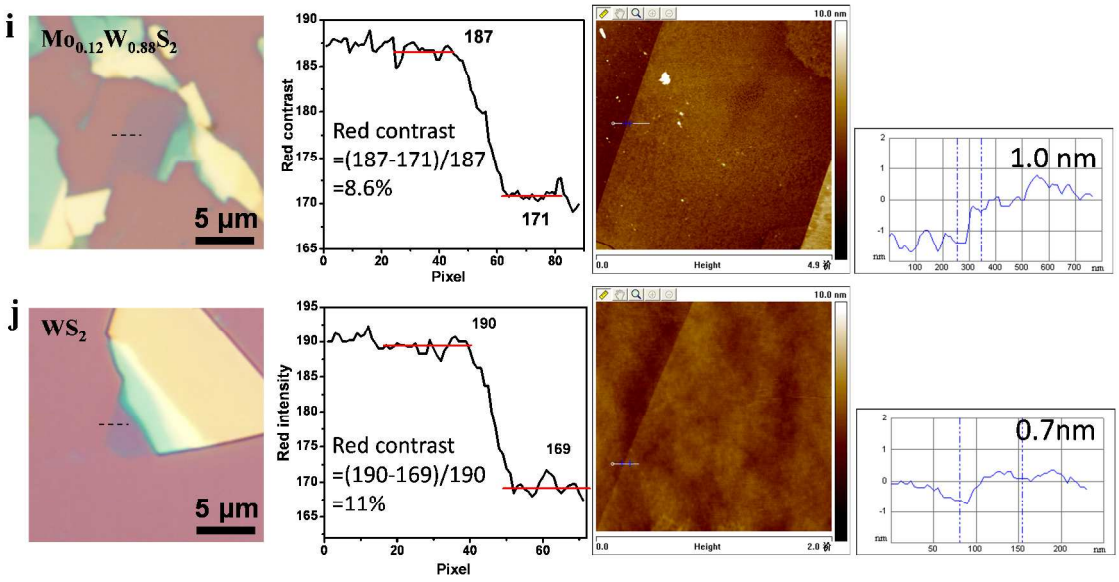

Figure S4. From left to right: optical image, section of red color intensity along the black dash lines, AFM image, AFM section analysis for (a) MoS_2, (b) $Mo_{0.87}W_{0.13}S_2$, (c) $Mo_{0.80}W_{0.20}S_2$, (d) $Mo_{0.71}W_{0.29}S_2$, (e) $Mo_{0.58}W_{0.42}S_2$, (f) $Mo_{0.39}W_{0.61}S_2$, (g) $Mo_{0.34}W_{0.66}S_2$, (h) $Mo_{0.23}W_{0.77}S_2$, (i) $Mo_{0.12}W_{0.88}S_2$, and (j) WS_2.

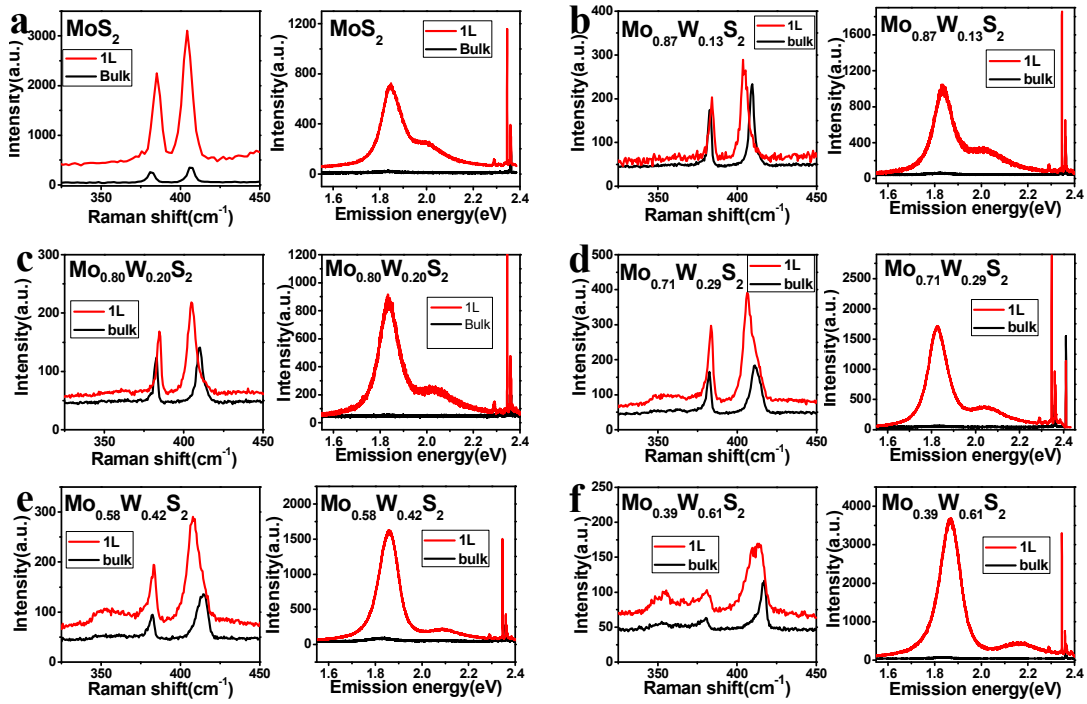

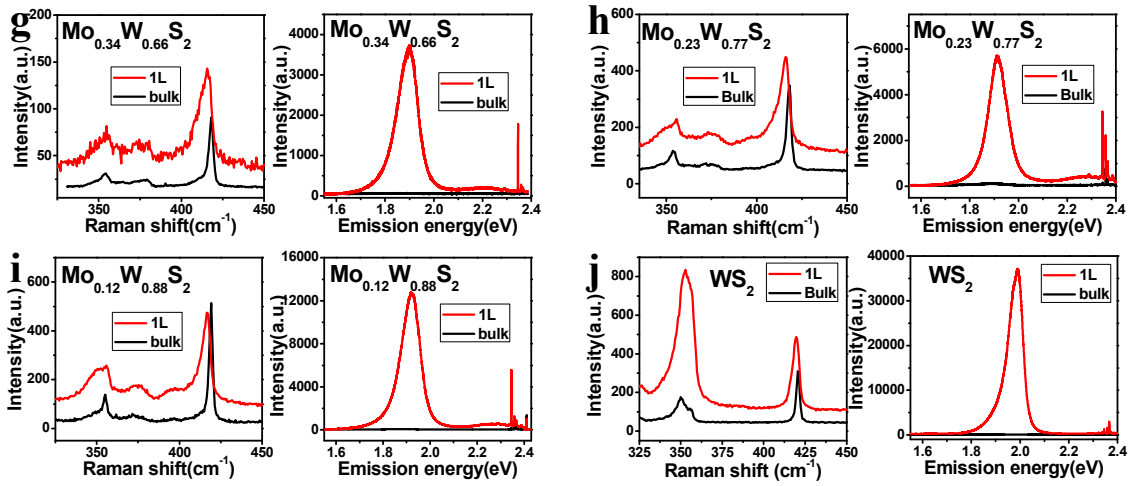

Figure S5. Raman and PL spectra of monolayer and bulk of (a) MoS_2, (b) $Mo_{0.87}W_{0.13}S_2$, (c) $Mo_{0.80}W_{0.20}S_2$, (d) $Mo_{0.71}W_{0.29}S_2$, (e) $Mo_{0.58}W_{0.42}S_2$, (f) $Mo_{0.39}W_{0.61}S_2$, (g) $Mo_{0.34}W_{0.66}S_2$, (h) $Mo_{0.23}W_{0.77}S_2$, (i) $Mo_{0.12}W_{0.88}S_2$, and (j) WS_2. All spectra were collected at 514.5 nm excitation.

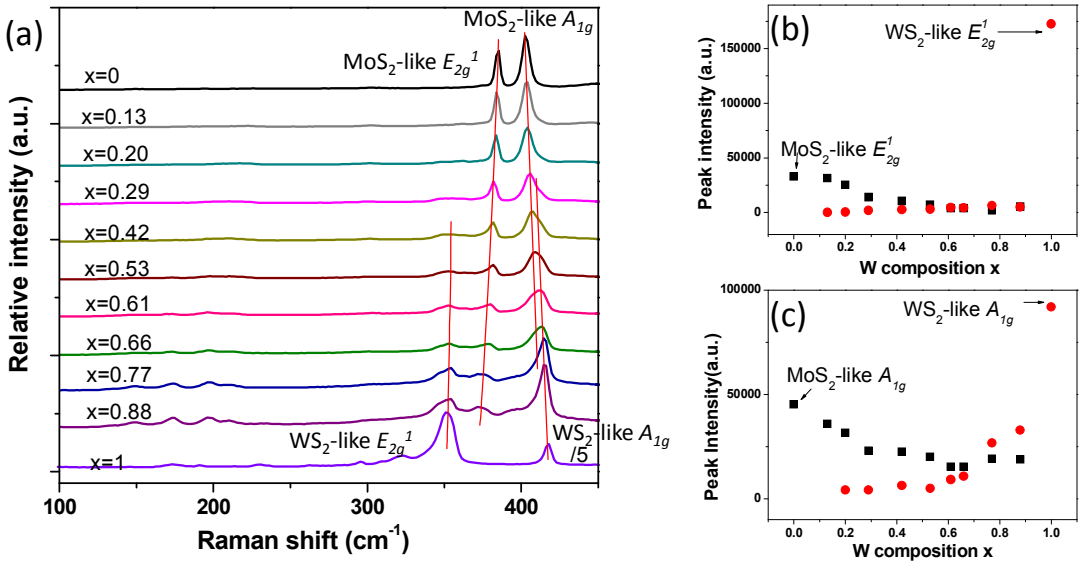

Figure S6. (a) Raman spectra of $Mo_{1-x}W_xS_2$ monolayers (at 514 nm excitation). Raman peak shift for E^1_{2g} and A_{1g} modes are indicated by red lines. Raman intensity changes for (b) E^1_{2g} and (c) A_{1g} modes (at 514 nm excitation).

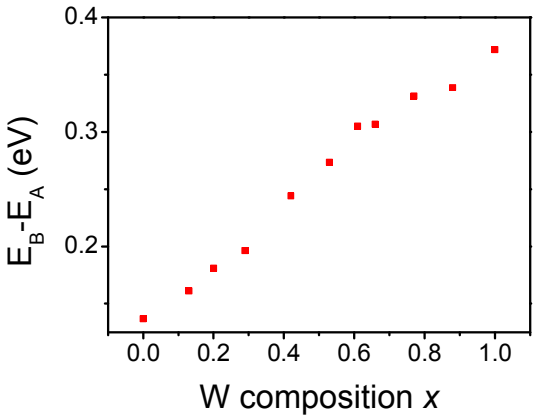

Figure S7. Energy difference between A and B exciton emissions at different W compositions.

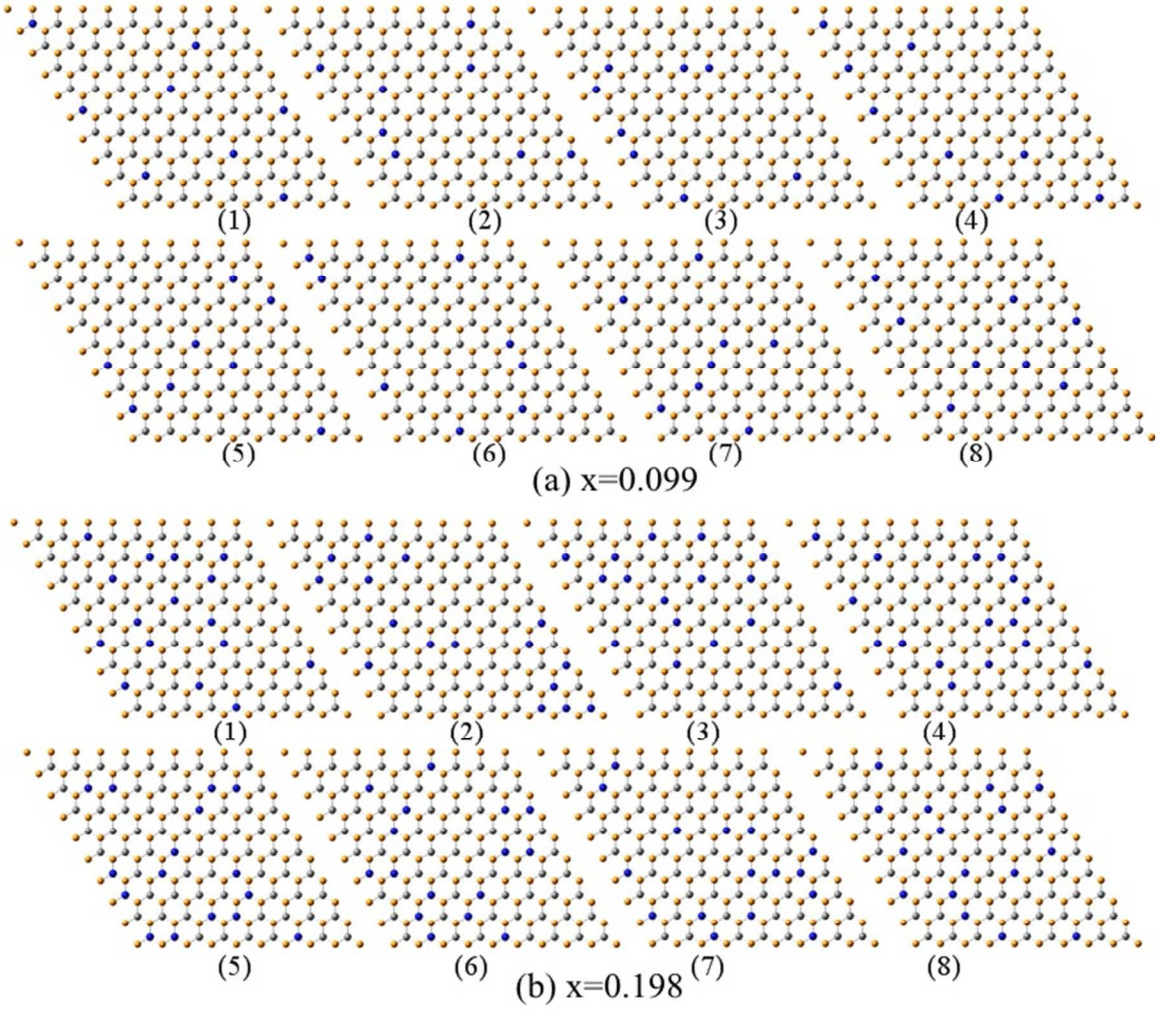

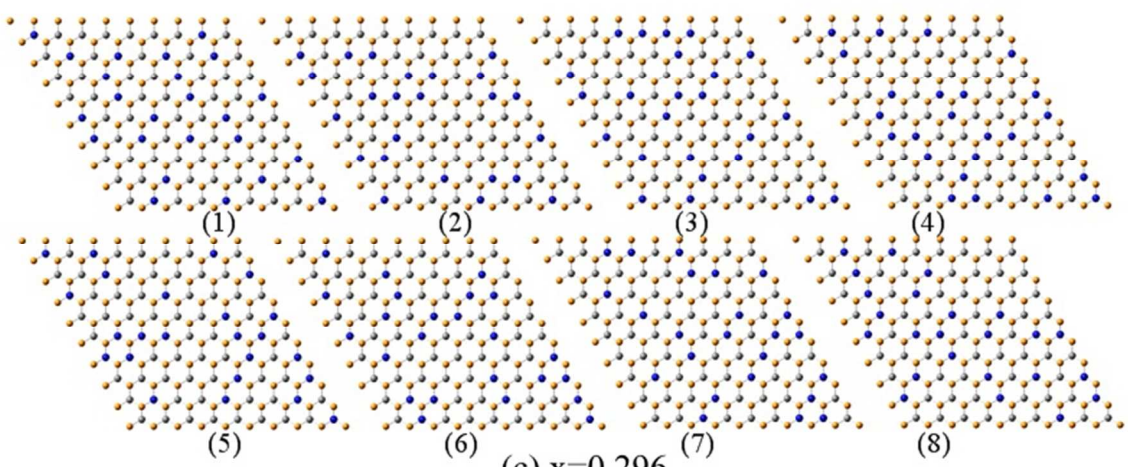

(c) x=0.296

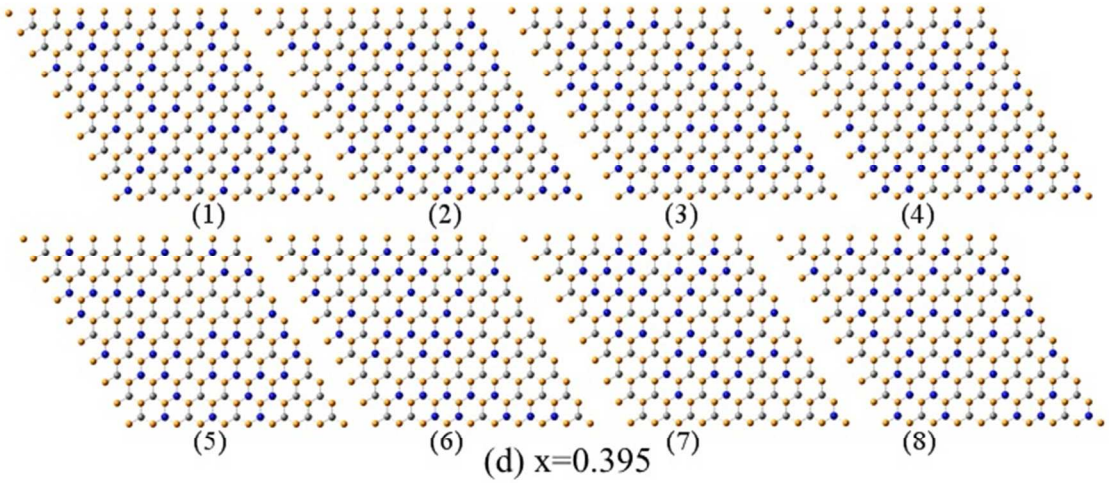

(d) x=0.395

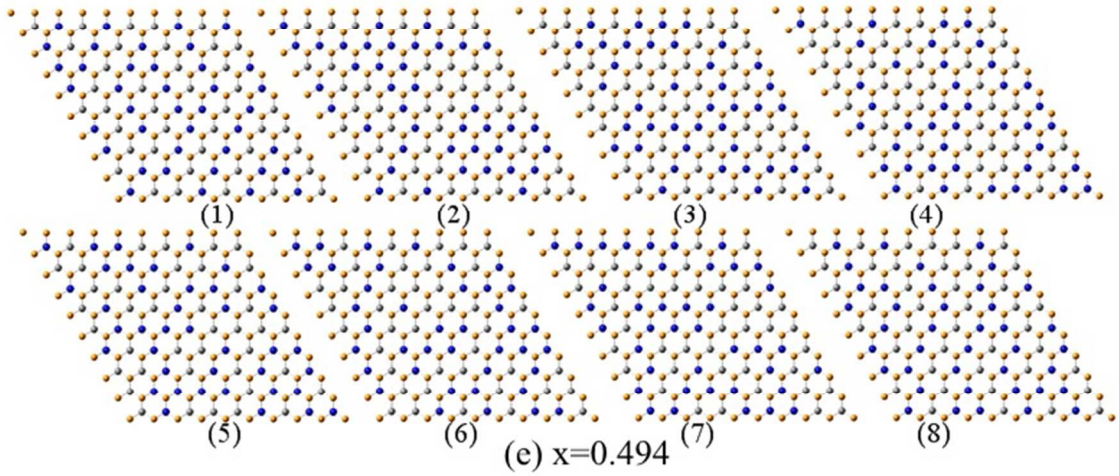

(e) x=0.494

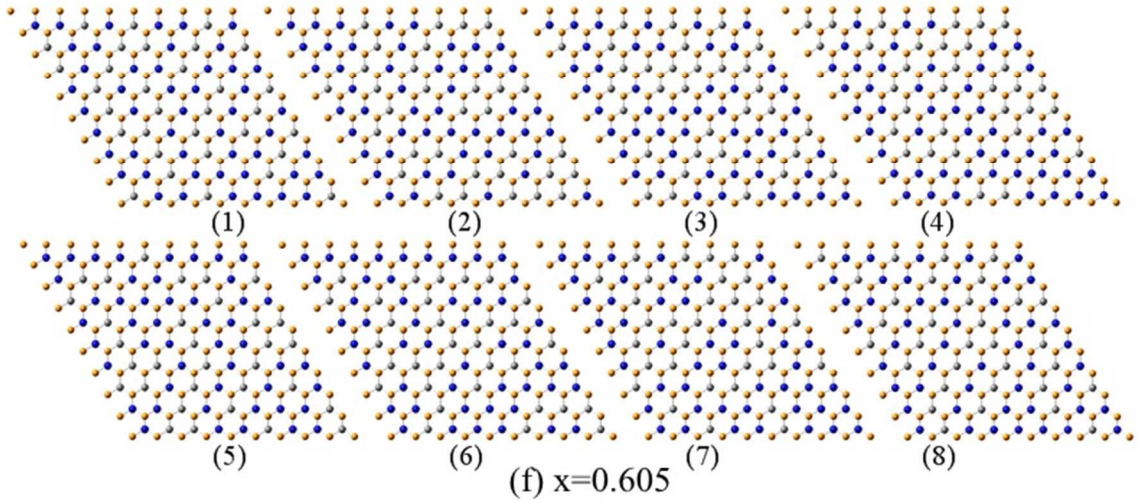

(f) x=0.605

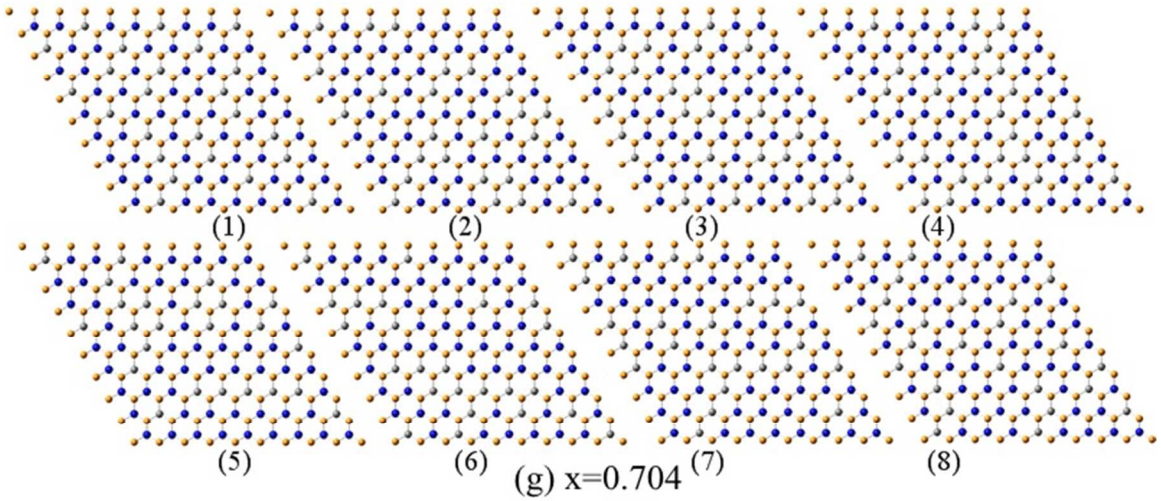

(g) x=0.704

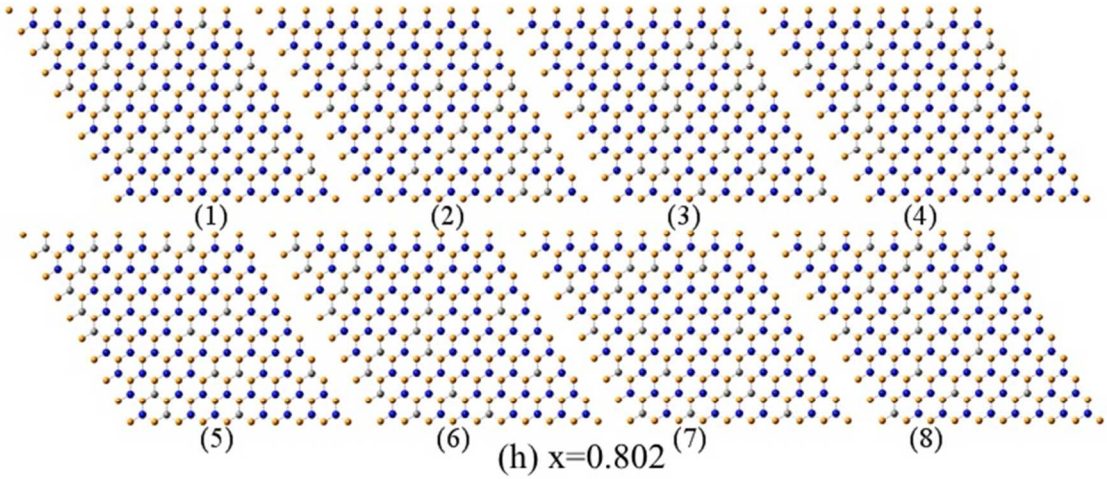

(h) x=0.802

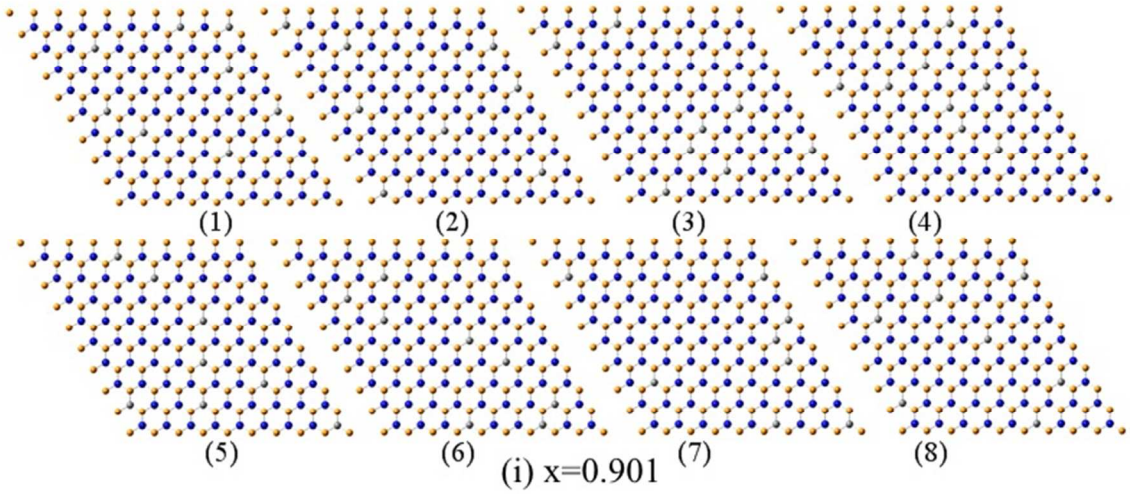

Figure S8. The 9×9 supercells at nine different W compositions *x* (except *x*= 0 or 1). For each *x*, there are eight random distributions of W atoms. The orange spheres represent S atoms, the gray spheres represent Mo atoms and the blue spheres represent W atoms.

Table S2. The vacuum energy level E_{vac}, the absolute energy levels of HOMO and LUMO as well as the band gaps E_g (in eV) for $Mo_{1-x}W_xS_2$ with different W composition *x*. The absolute energy levels of HOMO and LUMO were obtained by the approach of vacuum energy level calibration.

x	0.0	0.099	0.198	0.296	0.395	0.494	0.605	0.704	0.802	0.901	1.0
E_{vac}	2.377	2.384	2.390	2.396	2.403	2.409	2.417	2.423	2.430	2.436	2.442
HOMO	-6.119	-6.099	-6.079	-6.058	-6.038	-6.018	-5.995	-5.974	-5.954	-5.933	-5.911
LUMO	-4.328	-4.316	-4.295	-4.278	-4.252	-4.224	-4.194	-4.158	-4.118	-4.067	-3.975
E_g	1.791	1.784	1.783	1.780	1.786	1.793	1.801	1.816	1.836	1.866	1.936

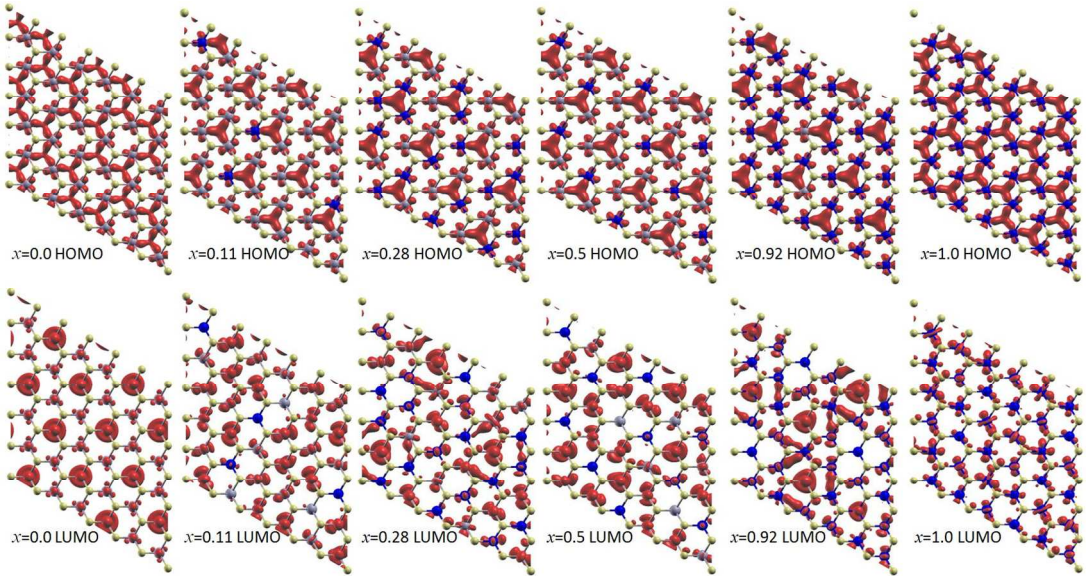

Figure S9. The charge density distributions of HOMO and LUMO for 6×6 supercells with six different W compositions *x*. The yellow spheres represent S atoms, the gray spheres represent Mo atoms and the blue spheres represent W atoms, respectively.

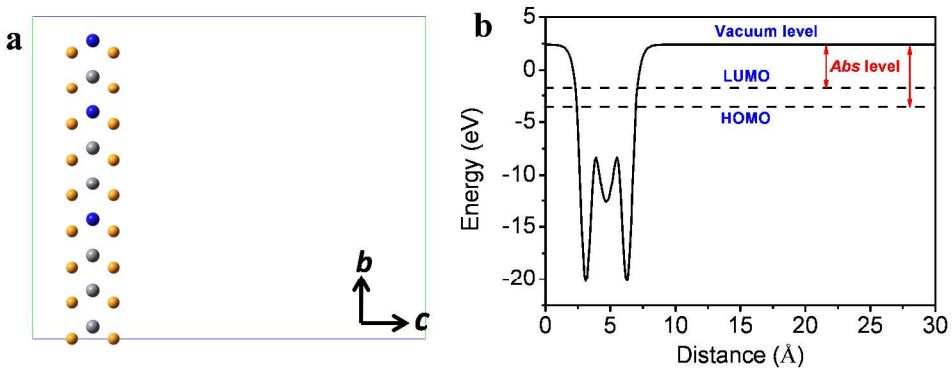

Figure S10. (a) The 9×9 supercell of $W_{0.5}Mo_{0.5}S_2$ in the *b*-*c* plane. The orange spheres represent S atoms, the gray spheres represent Mo atoms and the blue spheres represent W atoms, respectively. (b) The *a*-*b* plane averaged electrostatic potential along the *c*–axis direction. The flat line is the vacuum level, the upper dashed line is the LUMO position, the lower dashed line is the HOMO position. The absolute levels of HOMO and LUMO were obtained by the approach of vacuum energy level calibration.

Table S3. PDOS analysis of HOMO and LUMO. The ratio of each atomic orbital projected DOS to each element projected DOS for 6×6 supercells with nine different W composition *x*.

x	0.0		0.11			0.19			0.28			0.36			0.44			0.5			0.64			0.72			0.83			0.92			1.0	
	S	Mo	S	Mo	W	S	Mo	W	S	Mo	W	S	Mo	W	S	Mo	W	S	Mo	W	S	Mo	W	S	Mo	W	S	Mo	W	S	Mo	W	S	W
HOMO																																		
s	0	0.0004	0	0.0004	0.0005	0	0.0005	0.0005	0	0.0004	0.0004	0	0.0005	0.0006	0	0.0005	0.0006	0	0.0005	0.0005	0	0.0005	0.0006	0	0.0005	0.0005	0	0.0005	0.0006	0	0.0006	0.0007	0	0.0007
py	0.4995	0.0046	0.4989	0.0050	0.0055	0.4992	0.0054	0.0059	0.4981	0.0057	0.0055	0.4980	0.0058	0.0062	0.4980	0.0061	0.0066	0.4975	0.0064	0.0068	0.4984	0.0063	0.0077	0.4964	0.0067	0.0080	0.4986	0.0071	0.0084	0.4992	0.0070	0.0088	0.4996	0.0093
pz	0.0009	0	0.0021	0	0	0.0022	0	0	0.0035	0	0	0.0040	0	0	0.0042	0	0	0.0043	0	0	0.0040	0	0	0.0042	0	0	0.0024	0	0	0.0015	0	0	0.0008	0
px	0.4995	0.0046	0.4990	0.0050	0.0054	0.4985	0.0048	0.0079	0.4983	0.0054	0.0063	0.4979	0.0057	0.0065	0.4977	0.0059	0.0069	0.4981	0.0058	0.0073	0.4975	0.0068	0.0074	0.4993	0.0067	0.0079	0.4989	0.0074	0.0083	0.4992	0.0073	0.0088	0.4996	0.0089
dxy	_	0.4932	_	0.4932	0.4878	_	0.4928	0.4865	_	0.4984	0.4760	_	0.4950	0.4848	_	0.4938	0.4872	_	0.5002	0.4817	_	0.4762	0.4974	_	0.4812	0.4924	_	0.4822	0.4906	_	0.4903	0.4883	_	0.4875
dyz	_	0	_	0	0	_	0	0	_	0	0	_	0	0	_	0	0	_	0	0	_	0	0	_	0	0	_	0	0	_	0	0	_	0
dz^2	_	0.0038	_	0.0042	0.0051	_	0.0049	0.0043	_	0.0038	0.0055	_	0.0045	0.0061	_	0.0042	0.0062	_	0.0033	0.0064	_	0.0038	0.0058	_	0.0031	0.0062	_	0.0029	0.0049	_	0.0039	0.0051	_	0.0047
dxz	_	0	_	0	0	_	0	0	_	0	0	_	0	0	_	0	0	_	0	0	_	0	0	_	0	0	_	0	0	_	0	0	_	0
dx^2-y^2	_	0.4932	_	0.4922	0.4957	_	0.4916	0.4950	_	0.4863	0.4963	_	0.4885	0.4958	_	0.4895	0.4925	_	0.4839	0.4974	_	0.5064	0.4811	_	0.5018	0.4849	_	0.4999	0.4872	_	0.4910	0.4882	_	0.4889
LUMO																																		
s	0	0.0582	0.0312	0.0444	0.3455	0.0378	0.0369	0.1921	0.0240	0.0475	0.1473	0.0371	0.0349	0.1446	0.0451	0.0224	0.1306	0.0442	0.0227	0.1172	0.0436	0.0252	0.0863	0.0427	0.0221	0.0896	0.0448	0.0171	0.0801	0.0479	0.0060	0.0782	0.0568	0.0155
py	0.4977	0	0.4060	0.0019	0.0063	0.3564	0.0025	0.0041	0.4856	0.0015	0.0041	0.4586	0.0025	0.0083	0.3877	0.0043	0.0073	0.3465	0.0037	0.0064	0.3556	0.0033	0.0055	0.3680	0.0025	0.0053	0.3586	0.0019	0.0058	0.3978	0	0.0074	0.3936	0.0106
pz	0.0045	0	0.1083	0	0	0.1246	0	0	0.0864	0	0	0.1252	0	0	0.1536	0	0	0.1457	0	0	0.1457	0	0	0.1354	0	0	0.1398	0	0	0.1480	0	0	0.1865	0
px	0.4978	0.0018	0.4544	0.0021	0.0066	0.4812	0.0030	0.0090	0.4039	0.0012	0.0045	0.3790	0.0027	0.0051	0.4137	0.0039	0.0093	0.4636	0.0030	0.0104	0.4551	0.0025	0.0090	0.4539	0.0018	0.0076	0.4567	0.0018	0.0073	0.4063	0	0.0076	0.3630	0.0102
dxy	_	0.0015	_	0.0729	0.1023	_	0.0917	0.1098	_	0.0578	0.0751	_	0.1074	0.1730	_	0.1658	0.1656	_	0.1294	0.1510	_	0.1312	0.1437	_	0.1106	0.1383	_	0.0984	0.1601	_	0.0033	0.0044	_	0.3819
dyz	_	0	_	0	0	_	0	0	_	0	0	_	0	0	_	0	0	_	0	0	_	0	0	_	0	0	_	0	0	_	0	0	_	0
dz^2	_	0.9380	_	0.7961	0.3806	_	0.7454	0.4537	_	0.8512	0.6704	_	0.7555	0.5579	_	0.6354	0.4843	_	0.6973	0.4766	_	0.7129	0.5322	_	0.7647	0.5571	_	0.7750	0.5431	_	0.9882	0.4952	_	0.2206
dxz	_	0	_	0	0	_	0	0	_	0	0	_	0	0	_	0	0	_	0	0	_	0	0	_	0	0	_	0	0	_	0	0	_	0
dx^2-y^2	_	0.0018	_	0.0826	0.1589	_	0.1204	0.2313	_	0.0408	0.0986	_	0.0971	0.1111	_	0.1682	0.2030	_	0.1439	0.2384	_	0.1249	0.2234	_	0.0983	0.2021	_	0.1058	0.2037	_	0.0024	0.2072	_	0.3611